The speed of sound in (carbon dioxide + propane) and derived sound speed of pure carbon dioxide at temperatures between (248 and 373) K and at pressures up to 200 MPa

C.-W. Lin and J. P. M. Trusler*

Department of Chemical Engineering, Imperial College London, South Kensington Campus, London SW7 2AZ, U.K.

Abstract

The speed of sound in (carbon dioxide + propane) mixtures, with mole fractions of carbon dioxide between 0.938 and 0.998, has been measured at temperature from (248 to 373) K and at pressure between (8 and 200) MPa. We find that the addition of propane to carbon dioxide is highly effective in catalyzing vibration-translation energy transfer and reduces the sound absorption coefficient sufficiently to permit sensitive measurements of the speed of sound at frequencies in the low-MHz range. In this work, a 2 MHz ultrasonic cell based on the double-path pulse-echo method was used. The cell was calibrated with degassed ultrapure water at $T = 298.15$ K and $p = 1$ MPa, making use of the speed of sound computed from the International Association for Properties of Water and Steam equation of state (IAPWS-95). The estimated overall standard relative uncertainty of the speeds of sound measured in this study are 0.035 %. The speed of sound in pure carbon dioxide was obtained by extrapolation of the sound-speed data with respect to mole fraction at each experimental temperature and pressure. The average estimated overall standard relative uncertainty of the speed of sound in pure carbon dioxide obtained in this way is 0.1 %. Comparison of our results with speeds of sound computed from the equation of state of Span and Wagner suggest that the tolerance band of the latter may be reduced to 1 % at pressures up to 200 MPa.

Keywords: carbon dioxide; high pressure; propane; speed of sound, vibrational relaxation.

* To whom correspondence should be addressed. Tel: +44 (0)20 7594 5592, E-mail: m.trusler@imperial.ac.uk

1. Introduction

Liquid and supercritical carbon dioxide has been used in a wide range of industrial applications. For instance, it can be extracted from the atmosphere, used as a natural refrigerant, and released into the environment at end of life without detrimental effects.[1] In comparison with other commercial refrigerant, CO_2 has one of the lowest global warming potentials (GWP) and a high compression ratio. In recent decades, global warming associated with the emission of large amounts of CO_2 from the combustion of fossil fuels has been recognized as a major environmental challenge. To reduce anthropogenic CO_2 emissions in the next few decades to the agreed interim targets, carbon capture, transportation and storage are currently considered to be a key technology.[2] In this connection, it is important to know the thermodynamic and transport properties of both pure carbon dioxide and carbon dioxide containing various impurities, and there have been a number of studies extending over wide ranges of temperature and pressure.[3-7] In the design of pipeline transportation systems for compressed carbon dioxide, it is very important to model the propagation of shock waves in the fluid because of their important role in pipeline fracture mechanics. Knowledge of the decompression behavior of CO_2 is also important in connection with arresting fracture propagation. The role of impurities is crucial in pipeline failure scenarios and also in flow metering application. In these examples, the speed of sound of both pure and impure CO_2 is a key thermodynamic property.

Unfortunately, there are very few experimental studies of the speed of sound in liquid and super-critical CO_2. Among the few available studies are those of Herget,[8] and Pecceu and Van Dael[9] in the critical region. The only data available in a wide range of states are those of Pitaevskaya and Bilevich[10] which extend over the temperature range (273 to 473) K with pressures up to 450 MPa. However, the estimated relative uncertainty of these data is 2 %.[11]Additionally, a few high-precision data sets are available in the gas phase.[12-14] The *de*

facto equation of state (EoS) for carbon dioxide, due to Span and Wagner,[11] was therefore developed with very little sound-speed data[8, 10, 12, 14] and calculations of this property from the EoS have relatively high uncertainties amounting to 1.5 % or 2.0 % in the region of the present study. Thus, new and more accurate experimental sound-speed data would help in assessing the uncertainty of the Span-Wagner equation of state more rigorously than previously possible and ultimately may assist in the development of an improved EoS for CO_2. Additionally, sound-speed measurements for CO_2-rich mixtures could provide valuable information for the development of mixture models relevant to processes for CO_2 capture, compression, transportation and storage.

Sound-speed measurements in general have the advantages of rapidity, simplicity, and high accuracy. Thermodynamic integration of sound-speed data can be an excellent method of determining thermophysical properties.[15, 16] Once the speed of sound is known for all temperatures and pressures of interest, along with the values of values of density and isobaric heat capacity along an initial isobar, all observable thermophysical properties, including enthalpy increments, isochoric heat capacity and isothermal compressibility, can be calculated. In previous research,[16] fluids were typically studied at relatively high frequencies, normally $\geq$ 5 MHz; however, sound speed measurement in pure carbon dioxide are not possible at such high frequencies owing to an exceptionally high sound absorption coefficient which results in poor or no signal detection. In our case, using frequencies of 5 MHz or 2 MHz in pure CO_2 with path lengths of 40 mm and 60 mm in a pulse-echo experiment, no signal at all was detectable. Lowering the frequency by one order of magnitude did result in detectable signals and, as reported elsewhere,[17] a pulse-echo experiment operating at 500 kHz was partially successful in measurements of the speed of sound in pure CO_2 at temperatures from (263 to 363) K at pressures up to 325 MPa. However, overlap of echos and diffraction effects made the signals difficult to interpret and no reliable estimates of the experimental

uncertainty could be made. King et al.[18] have also made sound speed measurements in pure CO_2 using short path lengths and frequencies below 1 MHz. They used pulse correlation techniques to enhance the signal-to-noise ratio but did not tabulate numerical results or establish the experimental uncertainties. Our general conclusion is that it is extremely difficult to devise a method of measuring the speed of sound in pure CO_2 at high pressures with low uncertainty. Accordingly, an alternative approach is presented in this paper.

As detailed below, sound absorption in pure CO_2 is mainly associated with vibrational relaxation of carbon dioxide molecules; however, it can be greatly reduced by doping with a small amount of a suitably-selected component. The first objective of the present study was therefore to identify a suitable doping agent and thereby develop a methodology for measuring the speed of sound in slightly impure CO_2. Propane was identified as an effective doping agent, being non-toxic, non-corrosive, readily available in high chemical purity and miscible with CO_2 in the temperature and pressure ranges of interest. The second objective of this study was to measure the effect of propane as a doping agent on the speed of sound and, by means of extrapolation, to estimate reliable values for the speed of sound in pure CO_2 over wide ranges of temperature and pressure. This was accomplished by studying [x CO_2 + (1 − x) C_3H_8] at four mole fractions x between 0.938 and 0.998, temperatures between 248.15 K and 373.15 K and at pressures up to 200 MPa. The speeds of sound were extrapolate to limit x = 1 and compared with the values predicted for pure CO_2 by the equation of state of Span and Wagner. Although the present work extends to pressures much higher than encountered in typical industrial processes involving CO_2, it is helpful in the development of improved equations of state to have data over the widest possible range of thermodynamic states.

2. Sound absorption and dispersion in CO_2-rich mixture

In common with several other small rigid polyatomic molecules, carbon dioxide exhibits high sound absorption, associated with a long vibrational relaxation time, that renders precise measurements of the speed of sound difficult. From an acoustic point of view, the best approach is to employ a low-frequency measurement technique such that the period of the sound is much longer than the vibrational relaxation time; however, this implies using a large working volume of fluid, commensurate with the wavelength. In high pressure studies, it is difficult, and possibly unsafe, to use a large apparatus and, in the absence of excessive sound absorption, one would choose a high-frequency method with a small ultrasonic cell that can be contained safely within a pressure vessel of moderate dimensions. In this paper, we argue that an accurate measurement of the speed of sound in carbon dioxide can in fact be deduced from such high-frequency experiments by means of doping the CO_2 with a small amount of a suitable component that serves to catalyze vibration-translation energy transfer in the fluid and thereby reduce the sound absorption.

We first review the available data and models for vibrational relaxation in carbon dioxide and the associated sound absorption and dispersion. We then discuss the selection of a doping component with favorable acoustic and thermodynamic properties.

The analysis of vibration-translation energy transfer in pure CO_2 has generally be based on the assumption that the total vibrational energy of the molecule equilibrates with translations at a rate determined by a single relaxation time. In that case, the sound absorption coefficient α at frequency f is given approximately by[19]

$$\frac{\alpha}{f^2} = \left[\frac{\pi(\gamma-1)\Delta}{f_0 c_0}\right]\frac{1}{1+(f/f_0)^2}, \qquad (1)$$

where $\gamma = C_p/C_V$, C_p is the molar heat capacity at constant pressure, C_V is the molar heat capacity at constant volume, $\Delta = C_{vib}/C_p$, C_{vib} is the vibrational contribution to the molar heat capacity, c_0 is the speed of sound at zero frequency, $f_0 = [2\pi(1-\Delta)\tau_{11}]^{-1}$ is the appropriate relaxation frequency, and τ_{11} is the isothermal vibrational relaxation time. Furthermore, the speed of sound c at finite frequency is related to that at zero frequency as follows:[19]

$$\left(\frac{c_0}{c}\right)^2 = 1 - \left[\frac{(\gamma-1)\Delta}{(1-\Delta)}\right]\frac{(f/f_0)^2}{1+(f/f_0)^2}. \tag{2}$$

Thus, knowing Δ and τ_{11}, along with the necessary thermodynamic properties, one can compute both the dispersion and absorption arising from vibrational relaxation.

According to the kinetic theory of dilute gases, the vibrational relaxation time is inversely proportional to density and, for a pure substance, is given by

$$\tau_{11}^{-1} = (\bar{v}/\lambda)P_{11}^*, \tag{3}$$

where λ is the mean-free path, $\bar{v}$ is the mean molecular speed given by

$$\bar{v} = (8RT/\pi M)^{1/2}, \tag{4}$$

and P_{11}^* is the probability that a collision will give rise to vibration-translation energy exchange. In our analysis, which is intended only to provide a correlation of the available data, we approximate the mean free path with the elementary theory of hard spherical molecules, according to which:

$$\lambda = \left[\sqrt{2}\pi\sigma^2 n\right]^{-1}, \tag{5}$$

where σ is the molecular diameter and n is the number density.

At high densities, the molecular collision frequency is greater than that predicted by simple kinetic theory because of the finite volume excluded by the molecules. In their analysis of

vibrational relaxation in liquid and supercritical CO_2, Madigosky and Litovitz[20] found that the effective mean-free path in the dense fluid could be expressed as follows:

$$\lambda_{\text{dense}} = a\left[(1/n)^{1/3} - \sigma\right], \tag{6}$$

where a is a constant that we treat as an adjustable parameter. Madigosky and Litovitz found that their results were consistent with a hard-sphere diameter σ = 0.355 nm.

Vibrational relaxation times for CO_2 in the gas phase have been reported by several authors including Shields,[21] Estrada-Alexander and Trusler,[13] Merill and Amme,[22] and Lemming.[14] The results are in fair agreement at temperatures up to 450 K and, in figure 1, we plot the transition probabilities P_{11}^* determined from these data as a function of temperature under the assumption that σ = 0.355 nm. The data are represented in the temperature range from 220 to 450 K with the following empirical correlation:

$$P_{11}^* = 9.46 \times 10^{-6} \exp(T / 252\ \text{K}) . \tag{7}$$

Vibrational relaxation times in dense CO_2 have been reported by Bass and Lamb,[23] Henderson and Peselnick,[24] and Madigosk and Litovitz,[20] collectively covering temperatures between (273 and 323) K with densities up to almost 1200 kg·m^{-3}. To represent the high-density data, we fitted equation (6) to the results of Madigosk and Litovitz,[20] assuming that the transition probability remains the same as in the dilute gas, as found a = 1.852. In order to obtain a continuous representation of the vibrational relaxation time, we use equation (5) up to the density ρ_{cross} = 896 kg·m^{-3} at which the dilute-gas and dense-fluid expressions for the mean-free path cross, above which the latter is assumed to be valid. Although somewhat oversimplified, this approach is expect to provide a reasonable estimate of the vibrational-relaxation time in gas, liquid and supercritical states. Although related to compressed CO_2, the results of Bass and Lamb[23] and Henderson and Peselnick[24] all fall at densities below ρ_{cross} and hence they were not relevant to the estimation of the parameter a.

The high-density experimental data, along with relevant low-density results, are compared with the present model in Figure 2. The results of Henderson and Peselnick[24] at T = 323 K are scattered but agree with the model on the average, while those of Bass and Lamb[23] are between 7 % and 14 % greater than the model predicts. The measurements of Madigosk and Litovitz agree with our model to within ±7 %.[20] Overall, we conclude that the simple model outlined above provides a robust estimation of the vibrational relaxation time in pure CO_2 in gas, liquid and supercritical states at temperatures up to around 350 K.

We now have a basis for modelling the absorption and dispersion of ultrasound in pure carbon dioxide as functions of both frequency and the thermodynamic state of the fluid. In figure 3, we plot the absorption coefficient α as a function of T along isobars at pressures up to 200 MPa and at frequencies of (0.5, 1, 2 and 5) MHz. Detection thresholds corresponding to 90 % sound absorption over pathlengths of 5 mm and 50 mm are also shown and indicate that at frequencies above 1 MHz vibrational-relaxation gives rise to such high sound absorption that a sensitive measurement of the speed of sound would be impossible. At the lowest frequency considered, the sound absorption coefficient is small enough to consider a measurement in pure CO_2 with typical experimental pathlengths. However, as described above, our attempts to do this were only partially successful.

In mixtures of a relaxing substance, such as CO_2, with a non-relaxing additive the isothermal vibrational relaxation time is given by

$$1/\tau = x/\tau_{11} + (1-x)/\tau_{12}, \tag{8}$$

where τ_{11} is the relaxation time in the pure relaxing substance, x is the mole fraction of that substance, and τ_{12} is a relaxation time associated with unlike collisions. Certain additives, most notable H_2O, have a strongly catalytic effect associated with a very short relaxation time τ_{12} and, in such cases, the overall relaxation time can be much less than in the pure fluid even

at small values of $(1 - x)$.[25] Thus the addition of a suitable doping agent may reduce the relaxation time sufficiently to allow a sensitive measurement of the sound speed to be made at a frequency where the pure fluid alone would be acoustically opaque.

Although highly effective in catalyzing vibration-translation energy transfer for CO_2 molecules, H_2O is problematic as a doping agent: it is condensable, has limited miscibility in dense CO_2 and differs greatly from CO_2 in its thermodynamic properties. Light alkanes, on the other hand, are known to be effective in promoting vibration-translation energy transfer and have good miscibility with dense CO_2. As noted by Cottet *et al.*,[26] propane is especially suitable as it has almost the same molar mass as CO_2 and similar thermodynamic properties. Vibrational relaxation in (CO_2 + C_3H_8) mixtures has been studied at T = 298 K by Stephenson *et al.*[27] and, from their data and the present correlation for τ_{11}, we find that $\tau_{11}/\tau_{12} \approx 400$. The effect of this large ratio is to shorten of the overall relaxation time τ in mixtures with $(1-x) = O(10^{-2})$ sufficiently to permit sensitive sound speed measurements to be made over a large part of the liquid and supercritical-fluid regions at measurement frequencies in the low MHz range. To illustrate this, we plot in figure 4(a) the predicted sound absorption coefficient at a frequency of 2 MHz in a CO_2-rich mixture containing 1 mol% propane, assuming that $\tau_{11}/\tau_{12} \approx 400$ at all temperatures and pressures. Figure 4(b) shows the dispersion under the same conditions, plotted as $(c/c_0) - 1$, and we see that for states in which the sound absorption over a 50 mm path detection is below the indicated detection threshold the relative dispersion is less than 10^{-4} and thus negligible in the context of the present study. Analyses for other mole fractions of propane indicate that the dispersion is generally negligible under conditions in which a pulse is detectable after traversing a 50 mm path. In summary, we conclude that propane is an effective catalyst for vibration-translation energy transfer in CO_2 and that practical measurements should be unaffected by dispersion.

3. Experimental section

3.1 Material

Carbon dioxide was CP grade material supplied by BOC with a mole-fraction purity of 0.99995. Propane was supplied by Sigma-Aldrich with a mole fraction purity of 0.999. Deionized water with electrical resistivity > 18 MΩ·cm at T = 298 K was obtained from a Millipore apparatus. No further purification of any substance was attempted.

3.2 Experimental apparatus

The apparatus used in this work for fluids with high sound absorption was a modified version of the system described previously[16, 28, 29] operating at the lower frequency of 2 MHz. In this system, the dual-path ultrasonic cell shown in Fig. 5 was used in place of the 5 MHz cell used previously. This located within a high pressure stainless-steel pressure vessel immersed in thermostatic bath (Fluke model 6020) filled with silicone oil. The thermostatic bath provided a temperature stability and uniformity of ± 0.005 K over the entire study range. To achieve temperatures below ambient, a heat-exchanger device was immersed in the bath through which alcohol from an external refrigerated circulating bath was passed. The temperatures of the pressure vessel was measured with a platinum resistance thermometer (Fluke model 5615) with standard uncertainty u_T = 0.015 K. A pressure transducer (Honeywell model TJE/60000) used to measure the system pressure with an estimated standard uncertainty which was the larger of 0.05 MPa and $6\times10^{-4}p$. The fluid system, comprising a high-pressure syringe pump, pressure transducer, fill and drain valves and a rupture-disc safety device, was as described previously except for the addition of a circulation pump and a variable-volume pressurized sample storage vessel. The maximum working temperature and pressure of the apparatus were 473 K and 400 MPa, respectively.

3.3 Ultrasonic cell

The ultrasonic cell consisted of a piezoceramic transducer (PZT) made from lead zirconate titanate ($PbZrO_3/PbTiO_3$), two type 316 stainless-steel spacer tubes of unequal length and two type 316 stainless-steel reflectors. The 2 MHz PZT transducer, of 18 mm diameter and 8 mm thickness, was coated with gold on both surfaces to aid electrical contact and clamped between the spacer tubes with three 2 mm diameter threaded rods. These rods, located at an angle of $2\pi/3$ to each other, passed through the upper reflector and the shorter spacer tube and engaged threaded holes in the longer spacer tube. PEEK washers at the end of each rod and thin PTFE insulation sleeves were used to prevent a short circuit across the transducer. In addition, electrical connections were provided by a screw on the upper reflector and one of these rods.

To initiate a measurement, a function generator (Agilent 33120A) was used to generate a 10 V peak-to-peak five-cycle tone bust with a center frequency of 2 MHz. Therefore, two ultrasonic pluses propagated simultaneously in opposite directions along the fluid-filled paths. After being reflected at the ends of the acoustic path, these pulses returned to the PZT transducer where they were detected. The signal, comprising the initial tone bust and a set of echoes, was recorded by a high-speed digital oscilloscope (Agilent Technologies DSO6012A) with a bandwidth of 200 MHz and a sampling rate of 2 GHz and, from an analysis of the data,[28] the difference $(t_2 - t_1)$ between the round-trip times of flight on the long path, L_2, and short path, L_1, was calculated. The speed of sound was then obtained from the following simple relation

$$c = 2\Delta L / \Delta t \,, \tag{9}$$

where $\Delta L = (L_2 - L_1)$ and $\Delta t = (t_2 - t_1)$. Diffraction corrections, estimated by the method described previously,[16] were found to be smaller than the experimental uncertainty and were not considered further. In this study, the pathlength difference, ΔL was obtained by

calibration with degassed ultrapure water at a reference temperature T_0 = 298.15 K and reference pressure p_0 = 1 MPa. The speed of sound in liquid water in this reference state was obtained from the International Association for Properties of Water and Steam equation of state (IAPWS-95) and is associated with an uncertainty of 0.005%.[30] Variation of the pathlength difference with temperature and pressure was determined from the relation

$$\Delta L(T,p) = \Delta L(T_0,p_0)\{1+\langle\alpha\rangle(T-T_0)-\tfrac{1}{3}\beta(p-p_0)\} \quad (10)$$

where, $\langle\alpha\rangle$ is the mean value of the linear thermal expansivity α of type 316 stainless steel at pressure p_0 at temperatures between T_0 and T, and β is the isothermal compressibility β of type 316 stainless steel at temperature T, which we take to be independent of pressure. The linear thermal expansivity of the stainless steel was obtained by fitting the data given in reference [31] at $200 \leq T/\mathrm{K} \leq 500$ to the following Einstein function:[32]

$$10^6\alpha/\mathrm{K}^{-1} = a(\theta/T)^2\exp(\theta/T)/\{\exp(\theta/T)-1\}^2 \quad (11)$$

The resulting parameters were a = 1.686 and θ = 397.4 K. The isothermal bulk modulus $K = \beta^{-1}$ of the stainless steel can be represented as a quadratic polynomial in temperature:

$$K/\mathrm{MPa} = b_1 + b_2(T/T_0) + b_3(T/T_0)^2 \quad (12)$$

The parameters determined by fitting to the available literature data[31, 33] with T_0 = 298.15 K are b_1 = 234500, b_2 = 107800 and b_3 = 20300.

3.4 Variable volume cell and circulation pump

In order to measure the speed of sound in mixtures, such as the (CO_2 + C_3H_8) system studied in this work, that are not liquids under ambient conditions, a pressurized variable-volume cell is required to store the prepared mixture sample as a single homogenous liquid phase. A circulation pump is also used in the fluid system to homogenize the mixture after initial filling of the apparatus. The variable-volume vessel is shown in Fig.6. It was fabricated from

type 316 stainless steel, which exhibits a good combination of strength and corrosion resistance. The external dimensions of this vessel were length 22.9 cm and diameter 6.9 cm, the maximum internal volume of the sample chamber was 150 cm^3, and the maximum working pressure was 25 MPa at $T \leq 323$ K. A moveable piston divided the cylinder into two chambers: one for the sample and the other for the pressurizing medium which, in this work, was nitrogen gas regulated at a pressure of 12 MPa. The sample chamber also contained an agitator bar to aid initial homogenization by shaking. The mixture was prepared gravimetrically in the variable-volume vessel prior to injection into the speed of sound apparatus. Since, on initial filling of the evacuated apparatus, the sample would flash, a circulation pump was operated to re-mix the fluid and provide a homogenous state.

The circulation pump, rated for a maximum working pressure of 400 MPa, is shown in Fig 7. The pump cylinder was fabricated from a commercially-available high-pressure nipple, 100 mm in length, with an outside diameter of 14.3 mm, and an initial inside diameter of 4.8 mm. The internal bore honed to a final diameter of 5.00 mm so as to accommodate a cylindrical piston. The piston was fabricated from a magnetic stainless steel, type 431, and was 32 mm in length and 4.97 mm in diameter. The piston was drilled through to create an internal bore of 2 mm diameter, the top end was machined to form a 90° conical seat, and a 3 mm diameter ruby sphere was inserted above to create a check valve. A second check valve was fabricated from a 5.5 mm outside diameter tube with a similar conical seat and ruby-sphere seal. This was inserted into the top end of the nipple, which was counter-bored to accept the close-fitting check valve. A tubular stainless steel support was inserted below the piston to prevent it from falling to the bottom of the nipple. The piston was magnetically driven up and down by an external double solenoid coil, wound on an aluminum bobbin. The amplitude and the frequency of the sinusoidal driving current were regulated to obtain the desired flow rate.

3.5 Sample preparation

The mass of the variable volume cell was first measured on an analytical balance having a resolution of 0.001 g. Next, propane was injected and the mass measured again. Finally, liquid carbon dioxide was injected up to the desired pressure using a HPLC pump with refrigerated pump head. The mole fraction x of CO_2 in the mixture was computed from the relation

$$x = \left\{ \frac{(m_3 - m_2)}{M_1} \right\} \Big/ \left\{ \frac{(m_3 - m_2)}{M_1} + \frac{(m_2 - m_1)}{M_2} \right\}, \tag{13}$$

where m_1, m_2 and m_3 are the masses determined in the first, second and third weighings, and M_1 and M_2 are the molar masses of CO_2 and propane, respectively. Since the three weighings for each mixture preparation were completed within a short period during which the ambient air density was sensibly constant, buoyance corrections cancel. The standard uncertainty u_x of the mole fraction was calculated from the equation

$$u_x^2 = [(\partial x/\partial m_1)u_m]^2 + [(\partial x/\partial m_2)u_m]^2 + [(\partial x/\partial m_3)u_m]^2, \tag{14}$$

where the standard uncertainty of the mass, u_m, was taken to be 0.001 g. From this analysis, the standard uncertainty x was found to be 10^{-5}.

4. Results and discussion

4.1 Experimental results

The speed of sound in the mixtures of carbon dioxide with propane was measured along with six isotherms at nominal temperatures of (248.15, 273.15, 298.15, 323.15, 348.15 and 373.15) K and at pressure up to 200 MPa. Four compositions were measured with mole fractions x of CO_2 of 0.93757, 0.96828, 0.99073 and 0.99814. The minimum pressure on each isotherm varied and was determined by the point at which sound absorption became too

large for both echos to be clearly received. The measurements that were planned but not possible relate to mole fractions x = 0.96828, 0.99073 and 0.99814 at temperature of (298.15, 323.15, 348.15 and 373.15) K and pressure of (8, 15, 25) MPa. Additionally, the upper pressure bound at T = 248.15 K was limited by the freezing curve to less than 170 MPa for the same three compositions. The experimental results are listed in Tables 1 to 4.

The standard uncertainty u_c of the experimental speed of sound was estimated from the relation:

$$u_c^2 = \left[(\partial c/\partial T)_p u_T\right]^2 + \left[(\partial c/\partial p)_T u_p\right]^2 + \left[(\partial c/\partial x) u_x\right]^2 + (u_c^*)^2 , \quad (15)$$

where u_T, u_p, and u_x are the standard uncertainties of temperature, pressure and mole fraction discussed above, and u_c^* is the standard repeatability uncertainty, estimated to be $3.3 \cdot 10^{-4} c$. The overall standard relative uncertainty of c is then dominated by u_c^* and is approximately 0.035 % at all state points.

4.2 Derived speed of sound in pure carbon dioxide

The speed of sound in pure carbon dioxide was determined by extrapolation of the mixture data to the limit x = 1. To facilitate this, the data for each isotherm and each isopleth were first correlated as a function of pressure in terms of the relation:

$$(p - p_0) = a_1(c - c_0) + a_2(c - c_0)^2 + a_3(c - c_0)^3 , \quad (16)$$

where p_0 = 50 MPa and c_0 is speed of sound at $p = p_0$. The deviations from these correlation are plotted in Fig 8 and the average absolute relative deviation was found to be 0.04 %, which is similar to but slightly greater than the estimated standard relative uncertainty of the data. Equation (16), with the parameters pertaining to each temperature and composition, was then used to obtain the speed of sound at round values of the pressures equal to (8, 15, 25, 50, 75, 100, 125, 150, 175, 200) MPa. In order to interpolate these data to round values of the

temperature, quadratic (or in a few cases linear or cubic) polynomials in temperature were fitted for each pressure and composition and used to calculate the correction to be applied to refer each point to the desired temperature. This resulted in the interpolated data given in table 5. *T*, *p* states with data at fewer than three values of *x* were not considered as they would provide a reliable extrapolation to *x* = 1; such states are not included in Table 5. The lowest experimental temperature studied experimentally for the mixture with *x* = 0.99073 was inadvertently some 3 K above the nominal value and, in this case, we do not consider an extrapolation down to *T* = 248.15 K to be reliable. Accordingly, those data were not used further in the analysis. Finally, the corresponding speeds of sound in pure CO_2 were estimated by fitting the following quadratic function of mole fraction to the interpolated data at each temperature and pressure:

$$c(x) = c_0 + c_1(1-x) + c_2(1-x)^2 \tag{17}$$

Here, c_0 represents the speed of sound in pure CO_2. Figure 9, which shows the composition dependence of the speed of sound at each temperature and pressure, illustrates that the quadratic dependence upon mole fraction is justified by the data. The coefficients of equation (17) are given in table 5. The overall standard relative uncertainty of the speed of sound in pure carbon dioxide, also given in Table 5, was estimated by combining the standard relative uncertainty of the underlying experimental sound speeds, 0.035 %, with the relative standard deviation of c_0 determined in the regression analysis with equation (17). In a number of cases, data were available at only three mole fractions and, in those cases, the relative standard deviation of c_0 could not be calculated but was estimated to be 0.09 % (which is the mean values for the other states).

The ratio c_1/c_0 varies with the state point but, at the median temperature and pressure, it is approximately 0.3. This indicates that doping CO_2 with e.g. 1 mol% of propane, sufficient to

largely eliminate the deleterious effects of vibrational relaxation, will change the speed of sound by only about 0.3%. Thus when studying mixtures of CO_2 with substances, such as N_2, that do not catalyze vibration-translation energy transfer of CO_2 molecules, sound-speed measurements would be facilitates by adding a small amounts of propane and the necessary corrections for this are likely to be small.

4.3 Discussion

In Figure 11, we compare the speed of sound in the binary mixture with values calculated using the REFPROP 9.1 software.[34] These calculated values are based on reference-quality equations of state for CO_2 and C_3H_8,[11, 34] together with the GERG-2008 mixture model.[35] The predicted values are similar, but not identical, to those of the GERG-2008 because the pure-component equation of state used in REFPROP are more elaborate than those specified in GERG-2008. Furthermore, the GERG-2008 model is restricted to pressures not greater than 70 MPa. In the comparison with experiment, a clear trend emerges with the predicted values generally being too low at $p \leq 50$ MPa and generally too high are $p > 50$ MPa. Most of the deviations are within ±1 %. In Figure 12, we compare the present results for the speed of sound in pure CO_2 with the predictions of the EoS of Span and Wagner and find a similar pattern but with all deviations now within a band of ±1 %. These deviations are smaller than the tolerances of 1.5% to 2.0 % specified for the EoS of CO_2 in the temperature and pressure ranges of the present study but larger than the uncertainty of the present results. We also plot in Figure 12 the speeds of sound obtained earlier at $f = 0.5$ MHz[17] and find them to be in generally good agreement with the present data, although somewhat more scattered.

5. Conclusions

The speed of sound in (carbon dioxide + propane) has been measured at temperature between 248 K and 373 K, pressure up to 200 MPa and at four mole fractions of carbon dioxide spanning the range 0.937 to 0.998. The estimated overall relative uncertainty of the speed of

sound is approximately 0.035 %. From these data, we have estimated the speed of sound in pure carbon dioxide in the full temperature and pressure ranges with an average relative uncertainty of 0.1 %. Comparison with the EoS of Span and Wagner indicates that the tolerance band of the EoS for the speed of sound can be reduced to ±1 % in the temperature and pressure range of the present study. The sensitivity of the speed of sound in CO_2 to small amounts of C_3H_8 has been quantified.

References

(1) Lorentzen, G. Revival of carbon-dioxide as a refrigerant. *Int. J. Refrig.* **1994**, *17*, 292-301.

(2) Gibbins, J.; Chalmers, H. Carbon capture and storage. *Energy Policy* **2008**, *36*, 4317-4322.

(3) Zhao, Y.; Zhang, X.; Zeng, S.; Zhou, Q.; Dong, H.; Tian, X.; Zhang, S. Density, viscosity, and performances of carbon dioxide capture in 16 absorbents of amine plus ionic liquid + H_2O, ionic liquid + H_2O, and amine + H_2O Systems. *J. Chem. Eng. Data* **2010**, *55*, 3513-3519.

(4) Nourozieh, H.; Kariznovi, M.; Abedi, J. Measurements and predictions of density and carbon dioxide solubility in binary mixtures of ethanol and n-decane. *J. Chem. Thermodyn.* **2013**, *58*, 377-384.

(5) Sanchez-Vicente, Y.; Drage, T. C.; Poliakoff, M.; Ke, J.; George, M. W. Densities of the carbon dioxide plus hydrogen, a system of relevance to carbon capture and storage. *Int. J. Greenh. Gas Con.* **2013**, *13*, 78-86.

(6) Davani, E.; Falcone, G.; Teodoriu, C.; McCain, W. D., Jr. HPHT viscosities measurements of mixtures of methane/nitrogen and methane/carbon dioxide. *J. Nat. Gas Sci. Eng.* **2013**, *12*, 43-55.

(7) Al Ghafri, S.; Maitland, G. C.; Trusler, J. P. M. Densities of aqueous MgCl2(aq), CaCl2(aq), KI(aq), NaCl(aq), KCl(aq), AlCl3(aq), and (0.964 NaCl+00136 KCl)(aq) at temperatures between (283 and 472) K, pressures up to 68.5 MPa, and molalities up to 6 $mol.kg^{-1}$. *J. Chem. Eng. Data* **2012**, *57*, 1288-1304.

(8) Herget, C. M. Ultrasonic velcoity in carbon dioxide and ethylene in the critical region. *J. Chem. Phys.* **1940**, *8*, 537-542.

(9) Pecceu, W.; Van Dael, W. Ultrasonic velocity in liquid carbon dioxide. *Physica* **1973**, *63*, 154-162.

(10) Pitaevskaya, L. L.; Bilevich, A. V. Speed of ultrasound in carbonic-acid gas at pressures to 4.5 kilobars. *Russ. J. Phys. Chem. A* **1973**, *47*, 227-229.

(11) Span, R.; Wagner, W. A new equation of state for carbon dioxide covering the fluid region from the triple-point temperature to 1100 K at pressures up to 800 MPa. *J. Phys. Chem. Ref. Data* **1996**, *25*, 1509-1596.

(12) Novikov, I. I.; Trelin, Y. S. *Teploenergetika* **1962**, *9*, 79-84.

(13) Estrada-Alexanders, A. F.; Trusler, J. P. M. Speed of sound in carbon dioxide at temperatures between (220 and 450) K and pressures up to 14 MPa. *J. Chem. Thermodyn.* **1998**, *30*, 1589-1601.

(14) Lemming, W., *Experimentelle bestimmung akustischer und thermischer virialkoeffizienten von arbeitsstoffen der energietechnik*. VDI-Verlag: Deusseldorf, 1989; Vol. 32.

(15) Davis, L. A., Gordon, R. B. Compression of mercury at high pressure. *J. Chem. Phys.* **1967**, *46*, 2650-2660.

(16) Lin, C.-W.; Trusler, J. P. M. The speed of sound and derived thermodynamic properties of pure water at temperatures between (253 and 473) K and at pressures up to 400 MPa. *J. Chem. Phys.* **2012**, *136*, 094511.

(17) Lin, C.-W. Thermophysical properties of industrial fluids at high pressures from sound speed and density measurements. PhD, Imperial College London, 2014.

(18) Oag, R. M.; King, P. J.; Mellor, C. J.; George, M. W.; Ke, J.; Poliakoff, M.; Popov, V. K.; Bagratashvili, V. N. Determining phase boundaries and vapour/liquid critical points in supercritical fluids: a multi-technique approach. *J. Supercrit. Fluids* **2004**, *30*, 259-272.

(19) Matheson, A. J., *Molecular Acoustics*. Wiley-Interscience: London, 1971.

(20) Madigosky, W. M.; Litovitz, T. A. Mean free path and ultrasonic vibrational relaxation in liquids and dense gases. *J. Chem. Phys.* **1961**, *34*, 489-497.

(21) Shields, F. D. Thermal relaxation in carbon dioxide as a function of temperature. *J. Acoust. Soc. Am.* **1957**, *29*, 450-454.

(22) Merill, K. M.; Amme, R. C. Deactivation of the CO_2 bending mode by collisions with N_2 and O_2. *J. Chem. Phys.* **1969**, *51*, 844-846.

(23) Bass, R.; Lamb, J. Ultrasonic relaxation of the vibrational specific heat of carbon dioxide, sulfur hexafluoride, nitrous oxide, cyclopropane and methyl chloride in the liquid state. *Proc. Roy. Soc. London Ser. A* **1958**, *247*, 168-185.
(24) Henderson, M. C.; Peselnick, L. Ultrasonic velocity and thermal relaxation in dry CO_2 at moderate pressures. *J. Acoust. Soc. Am.* **1957**, *1074-1080*.
(25) Lewis, J. W. L.; Lee, K. P. Vibrational relaxation in carbon dioxide/water-vapor mixtures. *J. Acoust. Soc. Am.* **1956**, *38*, 813-816.
(26) Cottet, A.; Neumeier, Y.; Scarborough, D.; Bibik, O.; Lieuwen, T. Acoustic absorption measurements for characterization of gas mixing. *J. Acoust. Soc. Am.* **2004**, *116*, 2081-2088.
(27) Stephenson, J. C.; Wood, R. E.; Moore, C. B. Vibrational relaxation of laser-excited CO_2-polyatomic mixtures. *J. Chem. Phys.* **1972**, *56*, 4813-4816.
(28) Ball, S. J.; Trusler, J. P. M. Speed of sound of n-hexane and n-hexadecane at temperatures between 298 and 373 K and pressures up to 100 MPa. *Int. J. Thermophys.* **2001**, *22*, 427-443.
(29) Peleties, F.; Segovia, J. J.; Trusler, J. P. M.; Vega-Maza, D. Thermodynamic properties and equation of state of liquid di-isodecyl phthalate at temperature between (273 and 423) K and at pressures up to 140 MPa. *J. Chem. Thermodyn.* **2010**, *42*, 631-639.
(30) Wagner, W.; Pruss, A. The IAPWS formulation 1995 for the thermodynamic properties of ordinary water substance for general and scientific use. *J. Phys. Chem. Ref. Data* **2002**, *31*, 387-535.
(31) Kaye, G. W. C.; Laby, T. H., *Tables of physical and chemical constants and some mathematical functions 15th ed.* Longman London 1986.
(32) Ledbetter, H. M.; Weston, W. F.; Naimon, E. R. Low-temperature elastic properties of 4 austenitic stainless-steels. *J. Appl. Phys.* **1975**, *46*, 3855-3860.
(33) Grujicic, M.; Zhao, H. Optimization of 316 stainless steel alumina functionally graded material for reduction of damage induced by thermal residual stresses. *Mater. Sci. Eng. A-Struct. Mater. Prop. Microstruct. Process.* **1998**, *252*, 117-132.
(34) Lemmon, E. W.; McLinden, M. O.; Wagner, W. Thermodynamic Properties of Propane. III. A Reference Equation of State for Temperatures from the Melting Line to 650 K and Pressures up to 1000 MPa. *J. Chem. Eng. Data* **2009**, *54*, 3141-3180.
(35) Kunz, O.; Wagner, W. The GERG-2008 Wide-Range Equation of State for Natural Gases and Other Mixtures: An Expansion of GERG-2004. *J. Chem. Eng. Data* **2012**, *57*, 3032-3091.
(36) Lemmon, E. W.; Huber, M. L.; McLinden, M. O. *NIST Standard Reference Database 23: Reference Fluid Thermodynamic and Transport Properties-REFPROP, Version 9.1*, National Institute of Standards and Technology: Gaithersburg, 2013.

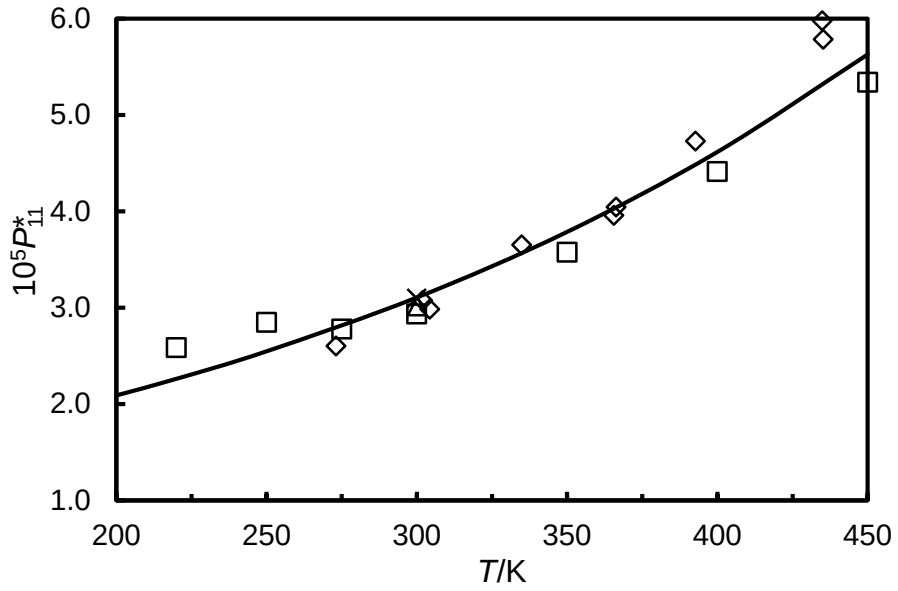

Figure 1. Vibration-translation transition probability P^*_{11} for CO_2 at temperature T: ◇, Shields;[21] □, Estrada-Alexanders and Trusler;[13] △, Merill and Amme;[22] ×, Lemming;[14] ——, equation (6).

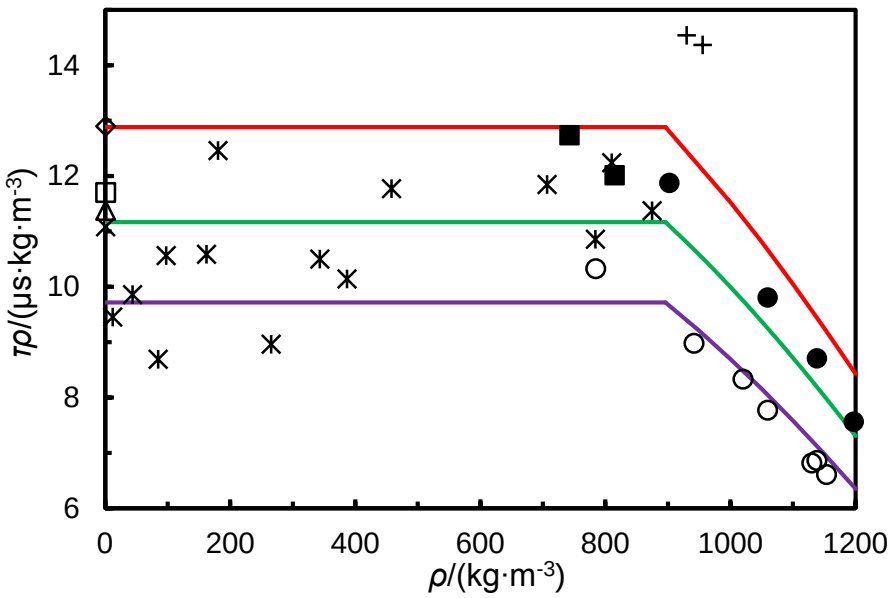

Figure 2. Relaxation time-density product $\tau\rho$ for CO_2 as a function of density ρ along three isotherms. Experimental data at T = 273 K: +, Bass and Lamb.[23] Experimental data at T =(298 to 300) K: □, Estrada-Alexanders and Trusler;[13] △, Merill and Amme;[22] ×, Lemming;[14] ■, Bass and Lamb;[23] ●, Madigosk and Litovitz.[20] Experimental data at T = 323 K: ∗, Henderson and Peselnick,[24] ○, Madigosk and Litovitz.[20] Solid lines: present model at temperatures, from the bottom, of 323 K (purple), 298 K (green) and 273 K (red).

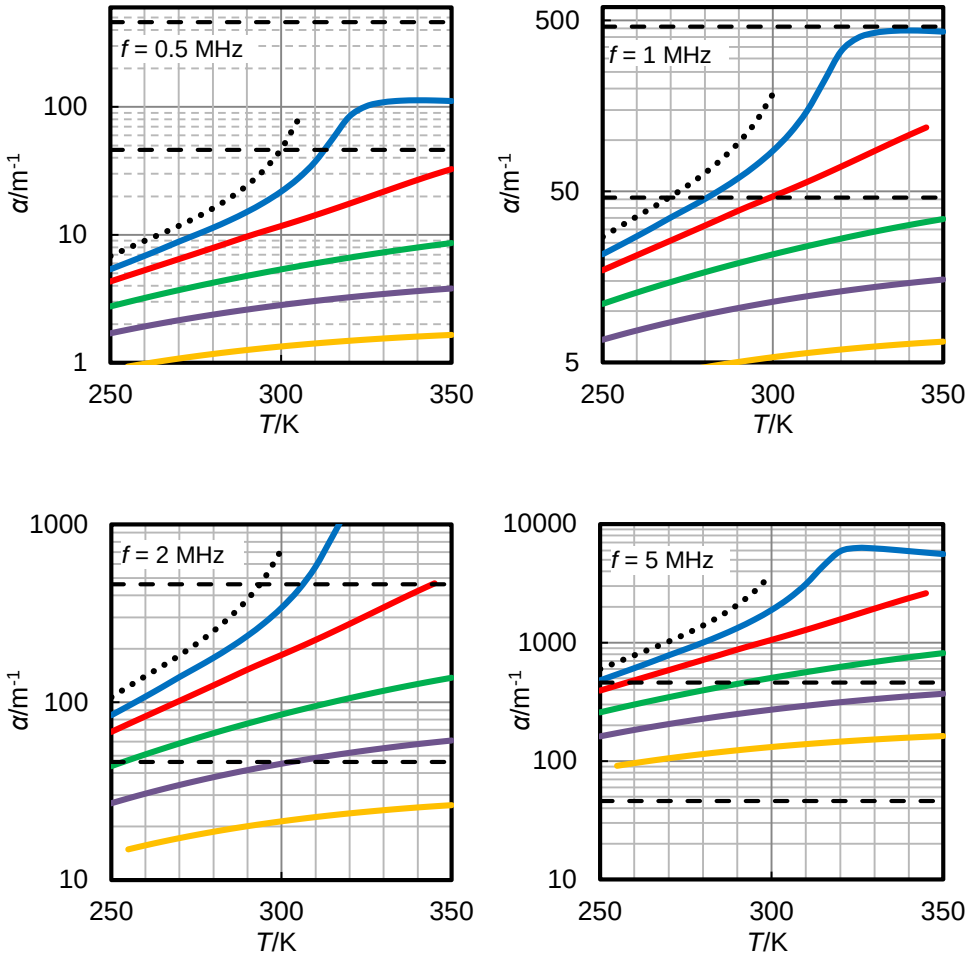

Figure 3. Ultrasound absorption coefficient α in pure CO_2 as a function of temperature T at various pressures p and frequencies f. From the bottom up: p = 200 MPa (yellow); p = 100 MPa (purple); p = 50 MPa (green); p = 20 MPa (red); p = 10 MPa (blue); …….. , saturated liquid; – – – – , detection limits (90 % absorption) for path lengths of 50 mm and 5 mm.

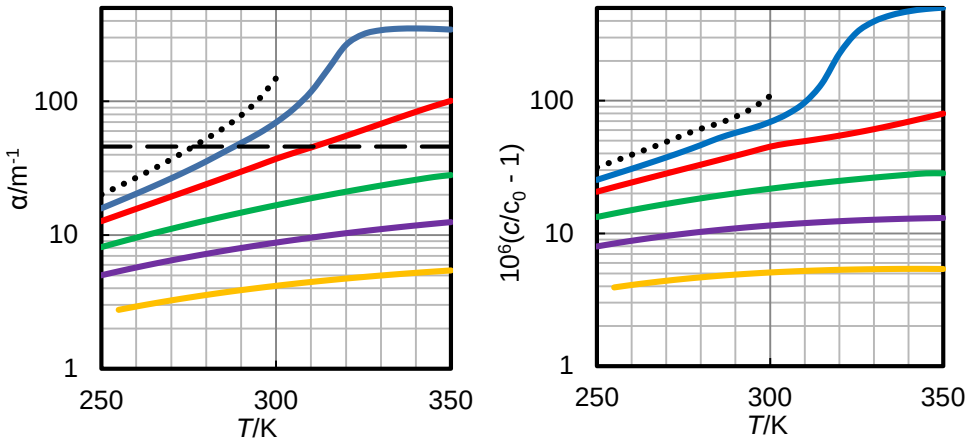

Figure 4. Predicted ultrasound absorption coefficient α and dispersion $[(c/c_0) - 1]$ at f = 2 MHz in the mixture (0.99 CO_2 + 0.01 C_3H_8) as a function of temperature T at various pressures p. From the bottom up: p = 200 MPa (yellow); p = 100 MPa (purple); p = 50 MPa (green); p = 20 MPa (red); p = 10 MPa (blue); ·····, saturated liquid.

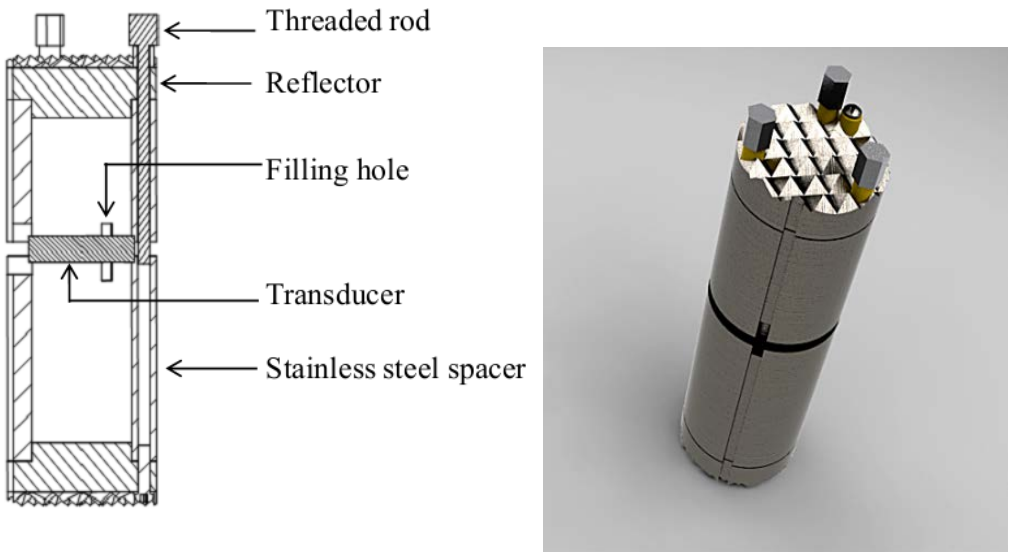

Figure 5. Cross-sectional and photographic views of the 2 MHz ultrasonic cell.

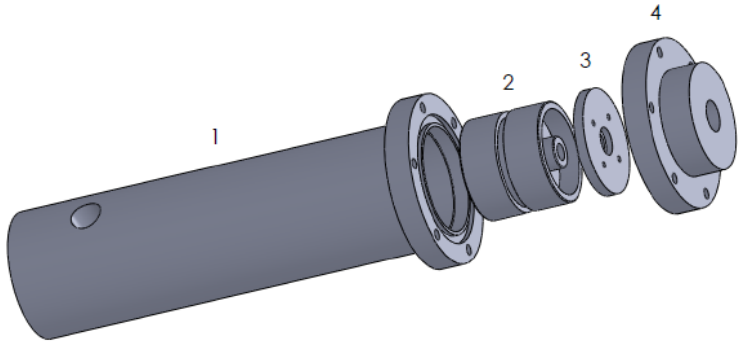

Figure 6. Exploded view of the variable volume cell showing: (1) blind cylinder with side-entry hydraulic pressure port and o-ring recess; (2) internal piston with o-ring recess; (3) piston retaining plate; (4) bolted end cap with pneumatic pressure port.

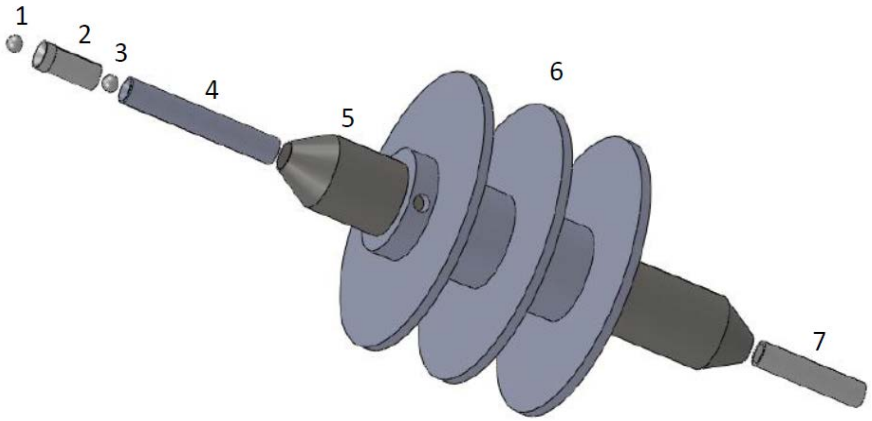

Figure 7. Exploded view of the magnetic circulation pump: (1) upper ruby ball; (2) fixed check valve body; (3) lower ruby ball ball; (4) magnet piston; (5) pump cylinder; (6) bobbin; (7) stainless steel support.

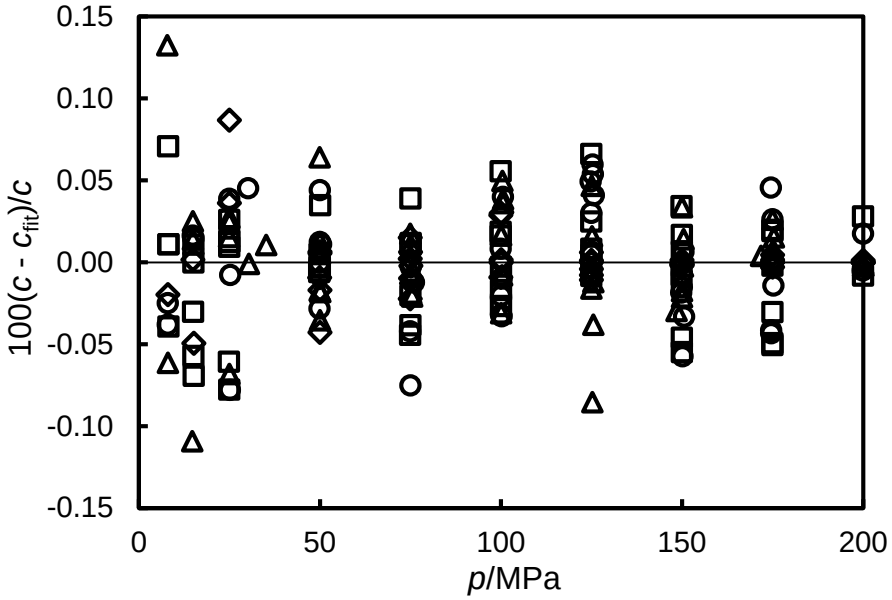

Figure 8. The deviations c - c_{fit} of experimental speeds of sound c from the values c_{fit} obtained from Eq. (16) with parameters fitted to the experimental data at each temperature and composition: □, x = 0.93757; △, x = 0.96828; ○, x = 0.99073;◇, x = 0.99814.

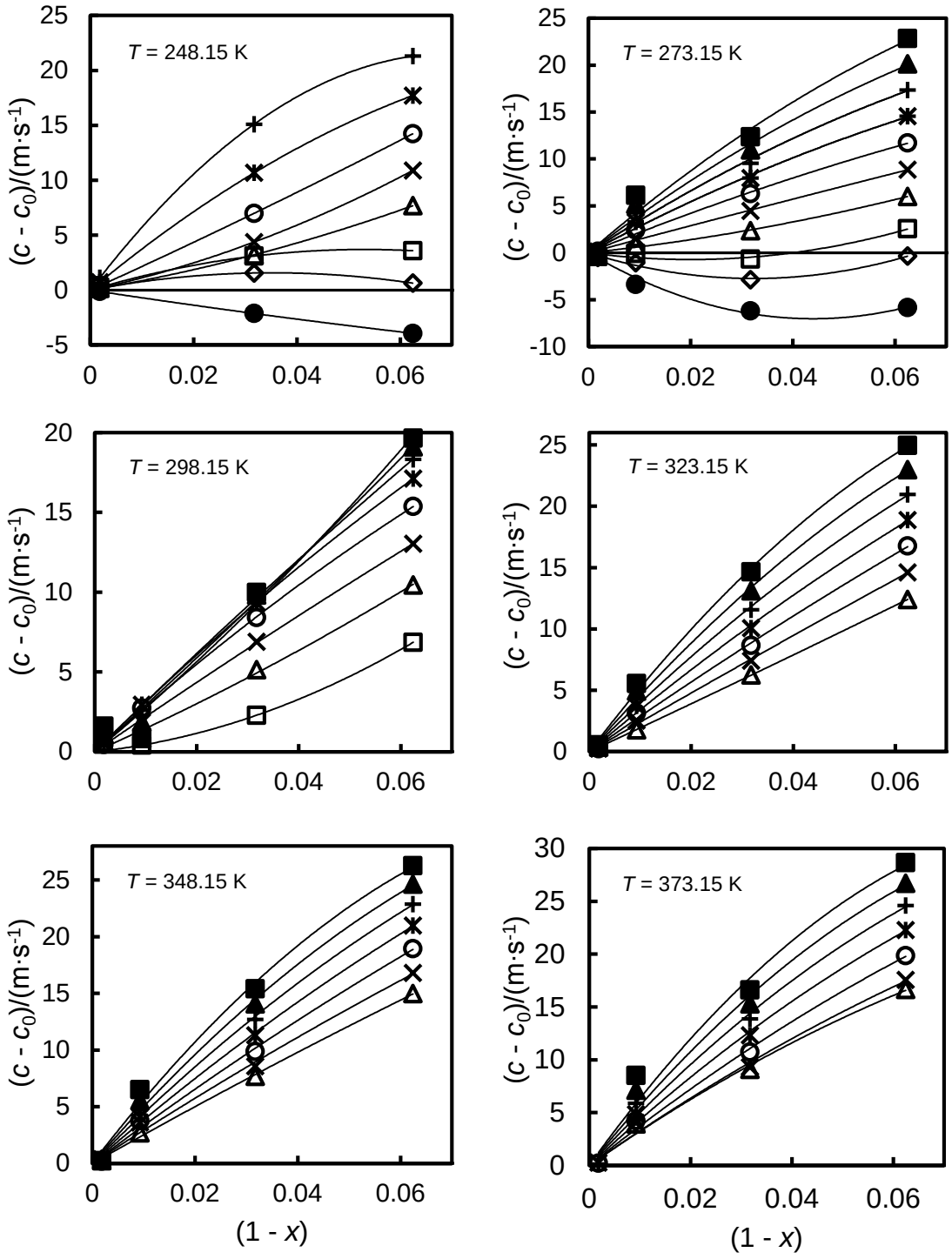

Figure 9. Differences ($c - c_0$) for [x CO_2 + (1 - x) C_3H_8] as a function of mole fraction x at temperatures T and pressures p, where c is the speed of sound and $c_0 = \mathrm{Lim}_{x\to 1}(c)$: ●, p = 8 MPa; ◇, p = 15 MPa; □, p = 25 MPa; △, p = 50 MPa; ×, p = 75 MPa; ○, p = 100 MPa; ∗, p = 125 MPa; ＋, p = 150 MPa; ▲, p = 175 MPa; ■, p = 200 MPa; ——, equation (17).

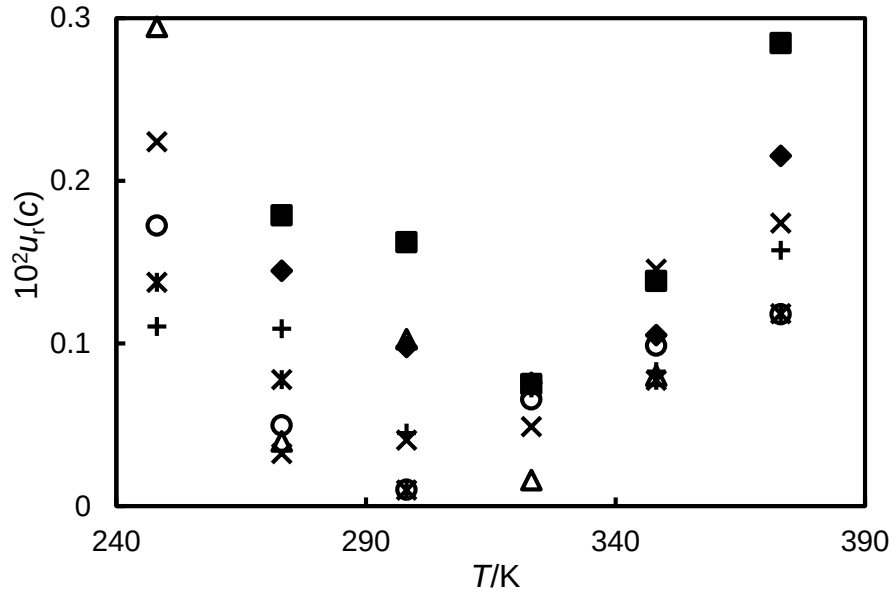

Figure 10. The overall relative standard uncertainty $u_r(c)$ of the speed of sound c in pure carbon dioxide as function as temperature T: △, p = 50 MPa; ×, p = 75 MPa; ○, p = 100 MPa; ∗, p = 125 MPa; +, p = 150 MPa; ◆, p = 175 MPa; ■, p = 200 MPa.

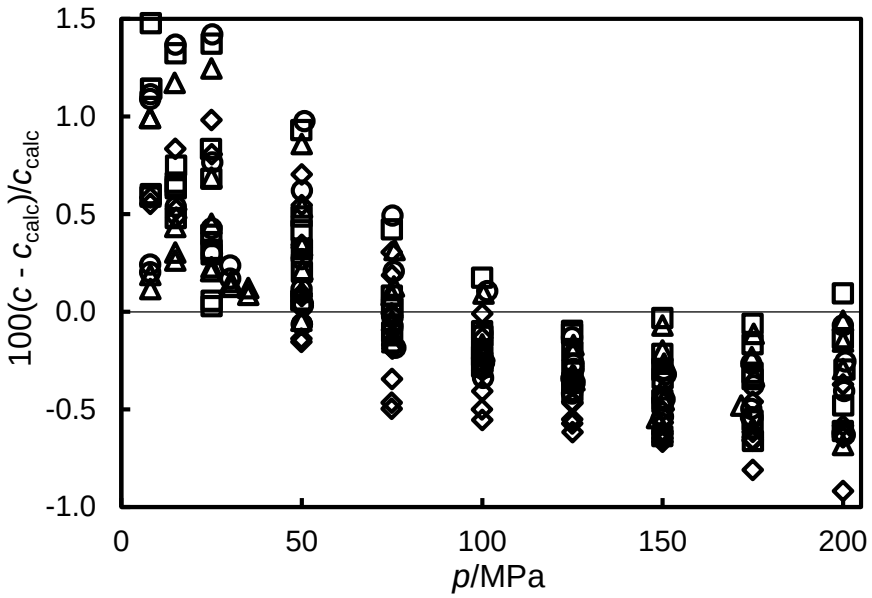

Figure 11. Relative deviations of experimental speed of sound c in [x CO_2 + (1 - x) C_3H_8] from the values c_{calc} calculated with the REFPROP mixture model[36] using the GERG-2008 mixing rules[35] as a function of temperatures T and pressures p: □, x = 0.93757; △, x = 0.96828; ○, x = 0.99073;◇, x = 0.99814.

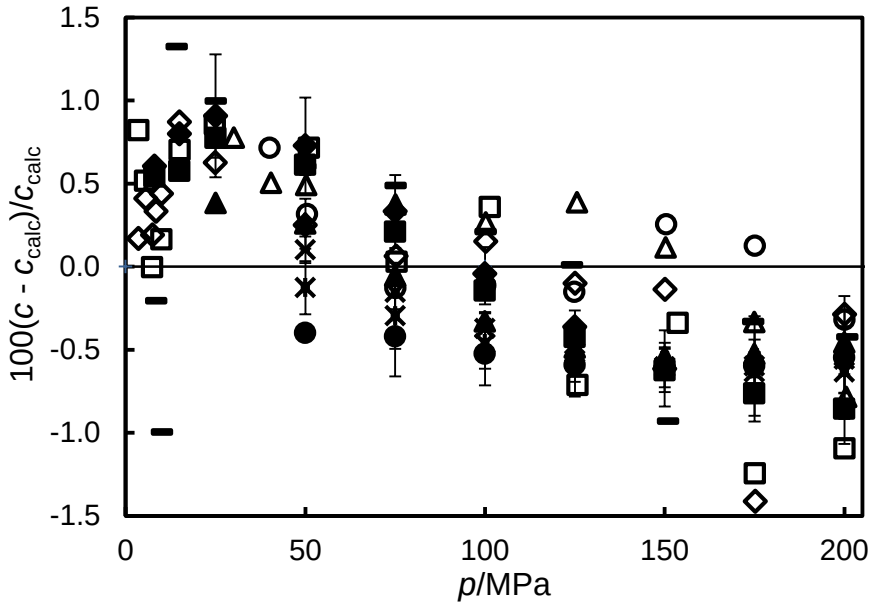

Figure 12. Deviations of the derived speeds of sound c in pure carbon dioxide from the values c_{calc} calculated from the equation of state of Span and Wagner.[11] This work: ◆, T = 248.15 K; ■, T = 273.15 K; ▲, T = 298.15 K; ×, T = 323.15 K; ∗, T = 348.15 K; ●, T = 373.15 K. Also shown are the experimental sound speeds measured at f = 0.5 MHz:[17] ◇, T = 263.23 K; □, T = 273.18 K; —, T = 303.15 K; △, T = 333.18 K; ○, T = 363.17 K.

Table 1. Speeds of sound c in [x CO_2 + (1 - x) C_3H_8] with x = 0.93757 at temperatures T and pressures p.[a]

p/MPa	c/(m·s^{-1})	p/MPa	c/(m·s^{-1})	p/MPa	c/(m·s^{-1})
T = 248.88 K		T = 298.18 K		T = 348.18 K	
8.27	799.4	8.21	388.5	25.05	446.8
15.03	855.4	15.12	538.7	50.05	682.3
25.03	924.8	24.99	659.0	75.10	830.6
49.91	1056.8	49.98	846.6	100.10	943.7
75.00	1159.3	75.09	975.1	125.02	1037.1
100.01	1246.2	100.01	1076.7	149.94	1117.7
125.00	1320.1	125.02	1162.3	174.97	1189.8
149.99	1385.8	149.96	1236.7	200.00	1254.3
174.98	1447.1	175.00	1302.7	25.04	446.6
8.27	799.4	200.10	1364.5		
		15.12	538.6		
T = 273.25 K		T = 323.19 K		T = 373.12 K	
8.18	614.8	15.16	381.4	25.06	385.0
15.19	699.7	25.00	541.2	49.89	618.8
24.92	787.4	50.09	758.5	75.09	772.6
50.00	946.5	75.07	897.6	100.00	889.4
75.02	1062.2	100.04	1005.2	124.97	985.6
100.04	1155.2	125.05	1095.7	149.93	1069.0
125.01	1236.3	150.02	1173.9	174.97	1141.6
150.00	1305.4	175.00	1243.4	200.03	1208.7
175.05	1369.6	200.42	1307.5	25.05	384.7
200.00	1428.5	15.12	381.2		
8.17	614.5				

[a] Standard uncertainties are u_T = 0.015 K, u_p = Max(0.05 MPa, $6\times10^{-4}p$) and u_c = 0.00035c.

Table 2. Speeds of sound c in [x CO_2 + (1 - x) C_3H_8] with x = 0.96828 at temperatures T and pressures p.[a]

p/MPa	c/(m·s^{-1})	p/MPa	c/(m·s^{-1})	p/MPa	c/(m·s^{-1})
T = 249.03 K		T = 298.14 K		T = 348.09 K	
7.92	797.2	14.96	532.2	30.40	504.8
14.79	852.8	24.98	654.5	50.03	675.2
25.01	922.3	50.05	841.6	75.22	823.0
49.98	1052.6	74.95	969.0	100.60	937.3
75.76	1155.3	100.06	1070.0	125.53	1029.0
100.41	1239.6	125.00	1154.1	150.44	1109.4
125.28	1312.1	150.29	1228.9	174.72	1178.6
150.01	1377.4	175.03	1294.1	200.04	1243.8
7.92	796.4	200.02	1354.1	30.39	504.8
		14.95	531.8		
T = 273.34 K		T = 323.09 K		T = 373.12 K	
8.01	610.5	24.94	534.8	35.17	488.8
14.92	694.4	50.14	752.6	49.95	611.6
25.00	785.0	75.00	890.2	75.07	764.5
50.05	942.8	100.59	1000.1	100.30	881.3
75.53	1058.9	125.56	1088.7	125.16	976.5
100.06	1149.4	75.07	897.6	150.00	1057.9
125.06	1229.3	149.97	1164.3	175.22	1131.5
148.51	1293.7	175.33	1234.8	200.01	1196.4
175.03	1360.3	200.00	1296.5	35.14	488.3
200.04	1417.3	24.93	534.6		
8.01	610.9				

[a] Standard uncertainties are u_T = 0.015 K, u_p = Max(0.05 MPa, $6\times10^{-4}p$) and u_c = 0.00035c.

Table 3. Speeds of sound c in [x CO_2 + (1 - x) C_3H_8] with x = 0.99073 at temperatures T and pressures p.[a]

p/MPa	c/(m·s^{-1})	p/MPa	c/(m·s^{-1})	p/MPa	c/(m·s^{-1})
T = 251.21 K		T = 298.13 K		T = 348.09 K	
8.05	786.8	25.18	653.9	50.37	672.7
15.01	844.2	50.02	837.8	75.08	816.9
25.27	913.8	75.23	965.0	100.58	931.1
50.77	1045.7	100.10	1064.0	125.70	1023.2
75.17	1143.2	124.97	1147.9	150.60	1101.4
101.43	1230.8	149.79	1220.2	175.29	1171.4
124.94	1299.1	174.53	1285.6	200.72	1236.7
150.91	1366.3	200.53	1346.2	50.36	672.7
8.12	787.6	25.11	654.1		
T = 273.39 K		T = 323.10 K		T = 373.13 K	
8.07	614.0	30.22	590.1	50.07	607.5
15.14	698.1	49.98	747.0	76.00	763.8
25.28	787.2	75.17	886.1	100.27	874.4
50.08	941.2	100.21	992.6	125.41	970.3
75.54	1055.9	124.81	1080.5	150.43	1051.5
100.08	1145.5	149.98	1157.2	174.66	1121.2
125.36	1225.5	174.62	1224.1	200.02	1188.3
150.17	1292.3	200.34	1288.4	50.05	607.3
174.97	1354.8	30.23	589.8		
199.91	1410.8				
8.05	613.9				

[a] Standard uncertainties are u_T = 0.015 K, u_p = Max(0.05 MPa, $6\times10^{-4}p$) and u_c = 0.00035c.

Table 4. Speeds of sound c in [x CO_2 + (1 - x) C_3H_8] with x = 0.99814 at temperatures T and pressures p.[a]

p/MPa	c/(m·s^{-1})	p/MPa	c/(m·s^{-1})	p/MPa	c/(m·s^{-1})
T = 248.59 K		T = 298.13 K		T = 348.09 K	
8.02	802.3	50.04	837.4	49.95	667.1
14.98	856.8	74.94	962.5	75.02	813.6
24.99	923.0	100.02	1061.9	99.98	924.6
50.04	1051.1	125.02	1145.5	124.98	1016.6
74.97	1149.9	150.01	1219.2	149.99	1095.6
100.01	1233.1	174.98	1285.5	175.00	1165.6
124.97	1303.8	200.01	1346.1	200.00	1228.6
150.04	1367.4	50.04	837.3	49.95	667.2
8.03	802.3				
T = 273.41 K		T = 323.13 K		T = 373.10K	
15.23	699.0	50.02	745.8	74.97	754.7
25.03	785.6	75.12	883.4	100.02	869.7
50.02	939.4	100.03	988.9	125.03	963.9
75.01	1052.3	124.98	1076.8	150.00	1044.4
100.02	1143.6	150.00	1153.2	175.00	1115.5
124.95	1220.2	175.02	1220.9	200.00	1179.3
150.01	1288.3	200.00	1282.1	74.95	754.4
174.99	1349.1	50.00	745.6		
200.00	1404.5				
15.20	699.0				

[a] Standard uncertainties are u_T = 0.015 K, u_p = Max(0.05 MPa, $6\times10^{-4}p$) and u_c = 0.00035c.

Table 5. Speeds of sound c in [x CO_2 + (1 - x) C_3H_8] and coefficients of equation (17) at temperatures T and pressures p; c_0 is the derived values of the speed of sound in pure carbon dioxide, and $u_r(c_0)$ is its overall standard relative uncertainty. [a]

T/K	p/MPa	c/(m·s^{-1})				c_0/(m·s^{-1})	c_1/(m·s^{-1})	c_2/(m·s^{-1})	$u_r(c_0)$
		x = 0.93757	0.96828	0.99073	0.99814				
248.15	8	801.81	803.61		805.61	805.74	-71	133	0.10%
248.15	15	860.23	861.16		859.76	859.60	89	-1272	0.10%
248.15	25	928.55	928.07		925.22	924.97	139	-1312	0.10%
248.15	50	1060.69	1056.22		1053.15	1053.00	79	708	0.10%
248.15	75	1162.80	1156.29		1152.10	1151.91	100	1191	0.10%
248.15	100	1248.21	1240.97		1234.37	1233.98	213	244	0.10%
248.15	125	1322.56	1315.51		1305.56	1304.84	391	-1717	0.10%
248.15	150	1388.94	1382.75		1368.77	1367.64	616	-4399	0.10%
273.15	8	612.51	612.17	614.99	618.25	618.36	-320	3648	0.15%
273.15	15	698.88	696.35	698.17	698.72	699.22	-170	2626	0.06%
273.15	25	789.06	785.84	786.42	786.09	786.50	-72	1802	0.08%
273.15	50	946.93	943.25	941.73	940.87	940.91	57	621	0.05%
273.15	75	1062.06	1057.65	1054.76	1053.32	1053.20	145	-56	0.04%
273.15	100	1155.63	1150.22	1146.34	1144.07	1143.93	221	-547	0.06%
273.15	125	1235.74	1229.16	1224.50	1221.27	1221.19	290	-933	0.08%
273.15	150	1306.45	1298.62	1293.33	1289.04	1289.09	355	-1250	0.11%
273.15	175	1370.15	1361.00	1355.21	1349.81	1350.03	413	-1492	0.14%
273.15	200	1428.39	1417.92	1411.69	1405.16	1405.56	470	-1720	0.17%
298.15	25	659.06	654.48	652.61		652.20	33	1231	0.10%
298.15	50	846.88	841.58	837.27	837.04	836.43	142	417	0.08%
298.15	75	975.14	969.00	963.98	962.63	962.11	221	-195	0.04%
298.15	100	1076.56	1069.58	1063.91	1061.63	1061.18	288	-662	0.04%
298.15	125	1162.02	1154.23	1147.83	1145.44	1144.90	317	-683	0.04%
298.15	150	1236.66	1228.11	1220.94	1219.11	1218.34	315	-329	0.05%
298.15	175	1303.41	1294.12	1286.14	1285.40	1284.30	288	311	0.09%
298.15	200	1364.08	1354.40	1345.28	1346.02	1344.42	266	829	0.16%
323.15	50	757.81	751.64	747.17	745.78	745.40	194	83	0.04%
323.15	75	897.28	890.09	885.20	882.93	882.67	242	-133	0.05%
323.15	100	1005.42	997.34	991.80	988.90	988.67	292	-385	0.07%
323.15	125	1095.60	1086.79	1080.45	1076.99	1076.71	349	-764	0.07%
323.15	150	1173.85	1164.44	1157.22	1153.23	1152.88	412	-1238	0.08%
323.15	175	1243.49	1233.60	1225.45	1220.95	1220.51	478	-1778	0.08%

323.15	200	1306.59	1296.29	1287.18	1282.19	1281.63	546	-2359	0.07%
348.15	50	682.08	674.78	669.80	667.33	667.10	255	-250	0.08%
348.15	75	830.12	821.87	816.92	813.28	813.32	296	-455	0.14%
348.15	100	943.42	934.35	928.23	924.67	924.48	339	-580	0.10%
348.15	125	1037.14	1027.44	1020.27	1016.51	1016.16	392	-913	0.08%
348.15	150	1118.02	1107.84	1099.87	1095.56	1095.14	454	-1417	0.08%
348.15	175	1189.71	1179.16	1170.63	1165.46	1165.09	520	-2038	0.10%
348.15	200	1254.46	1243.61	1234.71	1228.46	1228.21	590	-2741	0.13%
373.15	50	619.59	612.01	606.87	602.93	602.93	334	-1095	0.20%
373.15	75	772.21	763.98	758.71	754.62	754.66	336	-905	0.17%
373.15	100	889.16	880.04	873.52	869.51	869.30	382	-1041	0.11%
373.15	125	985.68	975.72	968.26	963.66	963.40	446	-1445	0.12%
373.15	150	1068.75	1058.03	1050.04	1044.30	1044.17	517	-2009	0.15%
373.15	175	1142.20	1130.78	1122.61	1115.36	1115.49	592	-2665	0.21%
373.15	200	1208.37	1196.32	1188.22	1179.21	1179.71	666	-3379	0.28%

[a] Relative standard uncertainties of *c* are 0.035 %.